© by PSP Volume 27 – No. 8/2018 pages 5285-5294 Fresenius Environmental Bulletin

CHARACTERISATION OF CELL SURFACES OF HOST WHEAT AND PATHOGENS (*TILLETIA FOETIDA* AND *TILLETIA CARIES*)

Ismail Poyraz[1,*], Zerrin Pat[2], Ahmet Umay[3]

[1]Department of Molecular Biology and Genetic, Faculty of Science and Letters, Bilecik Seyh Edebali University, 11230 Bilecik, Turkey
[2]Department of Chemistry, Faculty of Science and Letters, Bilecik Seyh Edebali University, 11230 Bilecik, Turkey
[3]Department of Test Research, Open Education Faculty, Anadolu University, 26470 Eskisehir, Turkey

ABSTRACT

Common bunt is one of the most destructive and dangerous among fungal wheat diseases. The most familiar species of this seed-born disease are *Tilletia foetida* and *Tilletia caries* and these two fungi cause significant yield losses worldwide. The virulence rate of a pathogen can change depending on the interaction with host cell surface. In this study, the characteristics of the cell surfaces of host wheat and two pathogens of disease were determined by scanning electron microscopy (SEM), zeta potential, optical tensiometer, attenuated total reflectance-Fourier transform infrared spectroscopy (ATR-FTIR) and thermogravimetric analysis (TGA). Two types of wheat samples (resistant M82-2161 and sensitive Heinles VII species) were used as the host cell. SEM analysis was performed at 4.00–5.00 KX and 77-79X magnification. Electrostatic charge is an important parameter for cell functions. The zeta potential was defined by a zeta sizer tool. Zeta potential values of these samples were defined as -43.9 to -4.46 mV. It was found that surface net charge plays an important role in host–pathogen interaction. The pathogens' charges were measured as more negative according to the host structure. The hydrophobicity of the Heinless VII and M82-2161 were very different, which is significant for pathogen–host interactions. The FTIR spectra showed differences between the pathogens and host. The thermal stability of all samples was examined using TGA. Results of this study demonstrate that surface charge, hydrophobicity and the surface molecules' structure of the plant and fungi cell wall play very important roles in host–pathogen interactions.

KEYWORDS:
Wheat, *Tilletia sp*, SEM, zeta potential, ATR-FTIR, thermogravimetry, contact angle

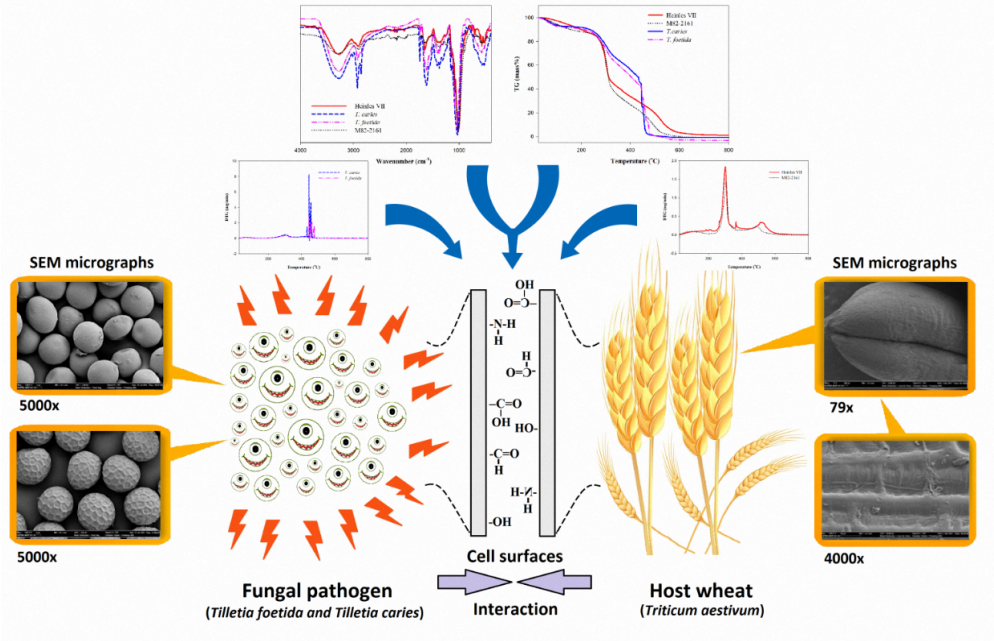

GRAPH 1
The characterization of cell surfaces to determine the interaction between host wheat and pathogen *Tilletia* sp.

INTRODUCTION

Fungal phytopathogens are the cause of most plant diseases [1]. Common bunt is a very important seed-borne disease in wheat farming and is the cause of serious economic losses [2-4]. Contamination of wheat with common bunt is a frequent cause of low-quality wheat production. Common bunt is caused by *Tilletia caries* (*T. caries*) (DC.) Tul., C. Tul. (1847) [syn.], *T. tritici* (Bjerk.) G. Winter [syn.] (1874) and *Tilletia foetida* (*T. foetida*) [Wallr.] Liro (1920) [syn.] *T. laevis* J.G. Kühn (1873) [2-8]. *Tilletia* pathogenic agents have the capacity to contaminate the wheat seeds in the field during harvesting by spores [9]. *T. foetida* and *T. caries* are mainly seed-borne pathogens replacing wheat grains in ears by smut balls consisting of teliospores on both spring and winter wheat [8, 9]. Recently, contamination of *T. foetida* and *T. caries* spores in wheat have become an especially major problem causing losses of yield and seed quality [4, 5, 7, 10].

Plants form physical and chemical barriers that cover their organs and function as protection against the hazardous external environment, including pathogenic attack. Plant–fungus interaction commences with the contact between the plant and spore surfaces [1]. The plant cell wall provides a physical and chemical barrier between pathogens and the internal contents of plant cells. The chemical composition and physical characteristics of the plant cell wall are an important factor in the outcome of the plant–pathogen interaction [11].

Chemical composition, topology and structures of the plant surface, as well as fungal spore shape, its texture and molecular features, influence the nature of the relationship [1]. The plant cell wall is also a highly dynamic structure that is constantly re-modelled during growth and development and in response to environmental cues [12]. Electrostatic charge is an important parameter for the cell functions [13]. The electric potential at the shear plane in the diffuse layer is known as the zeta potential. Measurements of electrophoretic mobility and electrostatic models have provided a wealth of insights into the binding of proteins, peptides and small molecules to lipid membranes. Some fundamental insights have permitted the study of the electrostatic binding of peptides, drugs, ions and other additives to membranes using zeta potential measurements [14]. Spectroscopic methods have also been applied in microbiology in different ways for quantitative and qualitative analysis and can fulfil these requirements [15].

Due to the specific and non-specific interactions of microorganisms, they bind to the host cell surface [16, 17]. The electric potential and hydrophobicity of the cell surface are often known as non-specific interactions. Proteins and mannoproteins are effective in the cell surface hydrophobicity of the fungal cell wall [17, 18]. These hydrophobic molecules play an important role in pathogenesis and adhesion morphogenesis because of the physical relationship between these hydrophobic molecules and hydrophilic regions of the host cell wall [17, 19-23].

The ATR-FTIR is an excellent tool for quantitatively analysing microstructural features [24]. FTIR spectroscopy is suitable for the identification of microorganisms and presents a new addition to existing taxonomic and genetic methods. The FTIR analysis of bacterial isolates provides fingerprint spectra, allowing the rapid characterisation of microbial strains. Additionally, the ATR-FTIR technique can be used for the observation of membranes [25].

TGA is one of the most commonly used thermal analysis techniques to study the thermal behaviour of biomass materials [26] and is faster, easier to implement and more cost-effective than existing wet chemical techniques [27]. It is successfully used to determine the amounts of hemicellulose, cellulose [27], lignin, xylan and other molecules in a biomass sample [28]. The virulence rate of pathogens changes depending on their interaction with host cell surface. In this study, the cell surfaces of wheat and two pathogens (*T. foetida* and *T. caries*) were characterised through SEM, zeta potential, optical tensiometer, ATR-FTIR and TGA analyses techniques.

MATERIALS AND METHODS

Selection and procurement of materials. All wheat (*Triticum aestivum*) and fungal (*T. foetida* and *T caries*) samples were obtained from Eskişehir Geçitkuşağı Agricultural Research Institute (EGARI), Eskişehir, Turkey (2015) and stored at room temperature. We selected a resistant (M82-2161) and a sensitive wheat variety (Heinles VII) for analysis. The virulence rates of pathogens were obtained from EGARI field studies.

Cell surface characterisation of the host wheat and pathogens. Host wheat and pathogen samples were characterised by SEM, zeta potentiometer, optical tensiometer, ATR-FTIR and TGA. Surface morphology of samples was performed using a scanning electron microscope (SEM-ZEISS Supra 40VP). SEM analysis was performed at 4.00–5.00KX and 77–79X magnification. All samples were coated with Platinum by Quorum-Q150Res Sputter Coater.

The cell surface charge of all samples was deduced from zeta potential analysis. The zeta potential of all samples was determined from their movement in the applied electrical field. The zeta potentials were defined at room temperature in distilled water with a Malvern-Nano ZS tool. The hydrophobicities of the host wheat surface were investigated by the measurement of water contact angles with an

optical tensiometer. Water contact angles were determined using an Attention Theta Lite Optical Tensiometer by the sessile drop method. One drop of water (~6µl) was dribbled upon host wheat and images of drops using the contact angles were determined by an image analysis program.

The ATR-FTIR spectrum of *T. foetida*, *T. caries* and the wheats were measured within the range of 4000–400cm^{-1} through the use of a Perkin Elmer-Spectrum100. Thermogravimetric analyses were performed using an Exstar TG/DTA7000 analyser series and samples were heated to a maximum temperature of 800°C at a heating rate of 10°Cmin^{-1}. Samples of about 7–12 mg were put in a ceramic pan and heated from room temperature to 800°C. The thermogravimetric data were automatically recorded and calculated with this thermal analysis software.

RESULTS AND DISCUSSION

Scanning electron microscopy (SEM). The first SEM analysis of the *Tilletia sp*. teliospore was performed by Mosse and Jones in 1968 and conducted only for description and classification [29]. However, no detailed SEM studies about *T. foetida* and *T. caries* have been conducted. The teliospore wall of *T. caries* is reticulated whereas that of *T. foetida* is smooth. Though morphologically different, the two species are similar in germination requirements and life cycle [4, 30]. At the same time, the virulence rates of the two pathogens differ from one another [10]. Therefore, it is important for the surface of the cell walls of both pathogens and hosts to be analysed. The SEM images of the samples are given in Figure 1 and Figure 2.

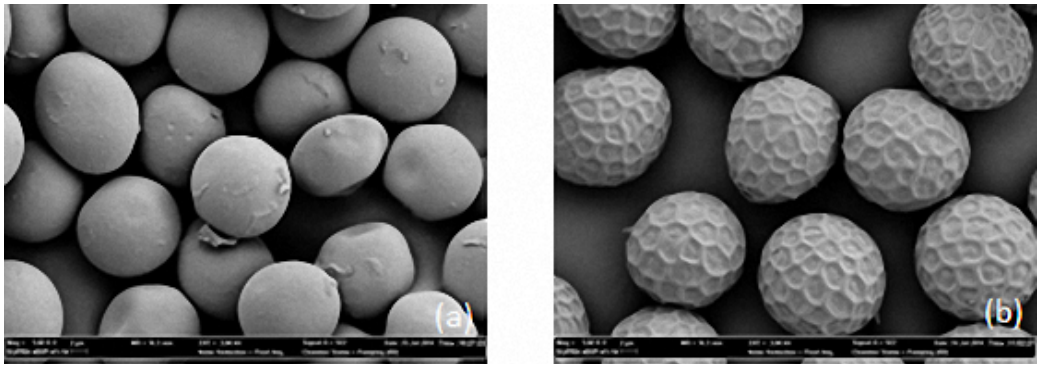

FIGURE 1
The 5000X SEM images of the fungal pathogens (a) *T. foetida* (b) *T. caries*

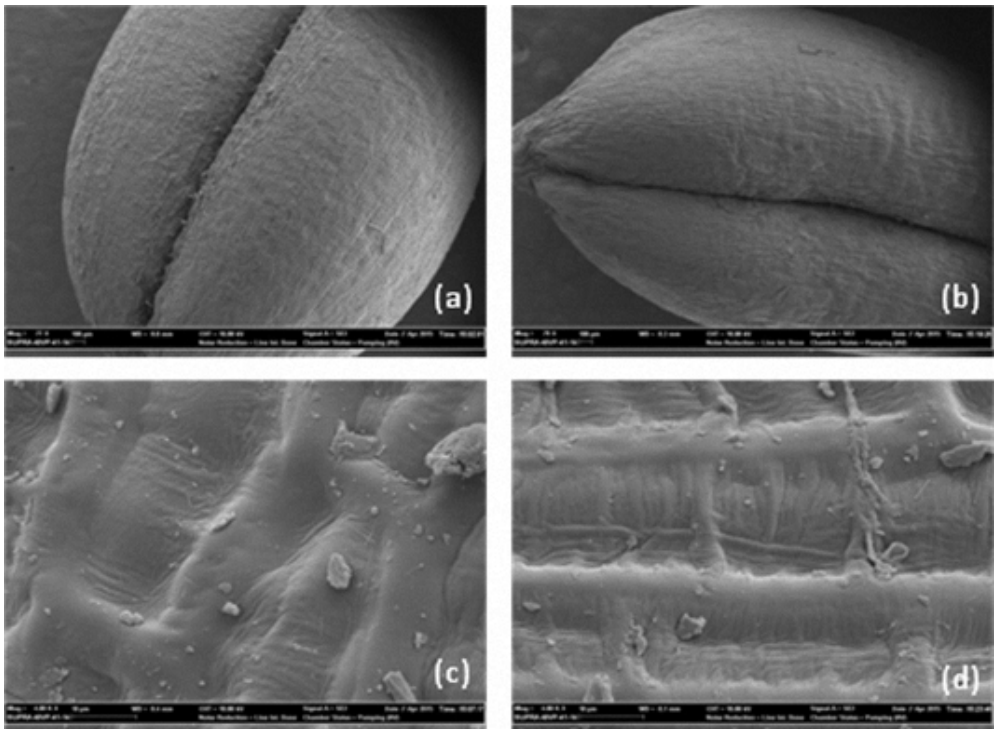

FIGURE 2
The SEM images of the wheat varieties (a) Heinles VII (sensitive) 77X, (b) M82-2161 (resistant) 79X, (c) Heinles VII surface 4000X, (d) M82-2161 surface 4000X

TABLE 1
The virulence rates, resistance rates and Zeta potential values of fungal pathogens (*T. foetida* and *T. caries*) and host wheats (sensitive Heinles VII and resistant M82-2161)

Pathogen	***Rate of disease (%)*** (for Heinles VII)	***Rate of disease (%)*** (for M82-2161)	***Zeta Potential (mV)***
T. foetida	*75*	*1,15*	*-29,20*
T. caries	*66*	*0*	*-43,90*
Host	***Resistance*** (for *T. foetida*)	***Resistance*** (for *T. caries*)	***Zeta Potential (mV)***
M82-2161	*Resistant*	*Resistant*	*-6,08*
Heinles VII	*Sensitive*	*Sensitive*	*-4,46*

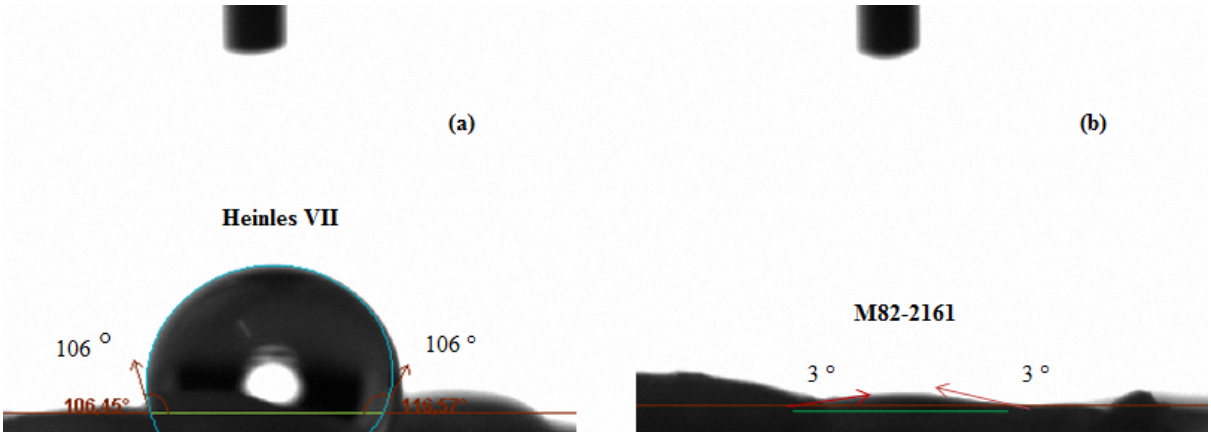

FIGURE 3
Contact angle images of the host wheat varieties (a) Heinless VII (sensitive) (b) M82-2161 (resistant)

The electron microscopy observations for *T. foetida* and *T. caries* showed the presence of surface differences between the pathogens in the SEM images. *T. caries* appears to be more uneven and jagged than *T. foetida*. The surface of both Heinles VII and M82-2161 wheat samples are porous and irregular.

Zeta potential analysis and pathogeny. The cell surface electrostatic charges of the pathogens and host cells were assumed to be equal to the zeta potential. Zeta potential measurements of pathogens and host cells were done in aqueous solution at room temperature. Under neutral conditions, the results showed that all pathogens and host cells are negatively charged (Table 1). The results showed that the pathogens are more negatively charged than the host cell. This information can be a basis for understanding adhesion and pathogeny.

Contact angle measurement. Pathogens–host interaction can be predicted according to surface free energy (SFE). SFE is related to the contact angle of the surface. When the SFE decreases, the hydrophobicities of the surface increases [31]. The hydrophobicities of the host cell surface are important for pathogen–host interaction because this structure must be a site of contact pathogen cells. The hydrophobicities of the cell surfaces were determined by the measurement of the contact angle (Figure 3).

In this study, two host cells were used, and host cell surfaces' hydrophobicities were investigated by contact angles measurements with water. The measured contact angle values of the host cells were very different from each other. The hydrophobic species was Heinless VII, which had a water contact angle of 106°, and the hydrophilic species was M82-2161, with a water contact angle of 3°. The cell surface of Heinless VII appears to have a high degree of hydrophobicity and this may be effective in fungal adhesion. Heinless VII is more vulnerable to pathogens and has disease rates higher than M82-2161 (Table 1).

Attenuated total reflectance-Fourier transform infrared spectroscopy (ATR-FTIR). The ATR-FTIR spectra of all samples are presented in Figure 4. The characteristic peaks for samples are shown in Table 2. The characteristic band at 1160 cm^{-1} is for antisymmetric stretching of C–O–C glycosidic linkages in both cellulose and hemicellulo [32-34] and C–H stretching assigned at 2889.2 cm^{-1}, and the peak at 723.0 cm^{-1} arises due to C–H bending of four or more methylene groups in the samples [35]. Aliphatic C–H stretching was assigned at 1370

cm^{-1} [25, 36, 37] and at 1650 cm^{-1} from C=O stretches in aryl ketones [25, 37, 38]. Xylan bands are found at 1245 cm^{-1} and 900 cm^{-1} [34, 39, 40]. Pectin bands at 1017 cm^{-1} and 1076 cm^{-1} β-(1→6) or β-(1→3) linked the galacton substrates. The characteristic band at approximately 1745cm^{-1} is for C=O ester stretching, lipids and carbohydrates, respectively. The band at 990cm^{-1}–702cm^{-1} consists of arabinoxylans and cellulose. The band at 3500–3300cm^{-1} is characteristic of OH–N–H stretching vibrations: carbohydrates and proteins [41-46].

Thermogravimetric analysis. TGA is used to determine how the thermal properties of samples vary with temperature [47]. The curves of thermogravimetry (TG) and derivative thermogravimetry (DTG) are presented in Figure 5 and Figure 6. The results of TG analysis, during the experimental procedures heating rate of 10° $Cmin^{-1}$, are shown in Figure 5.

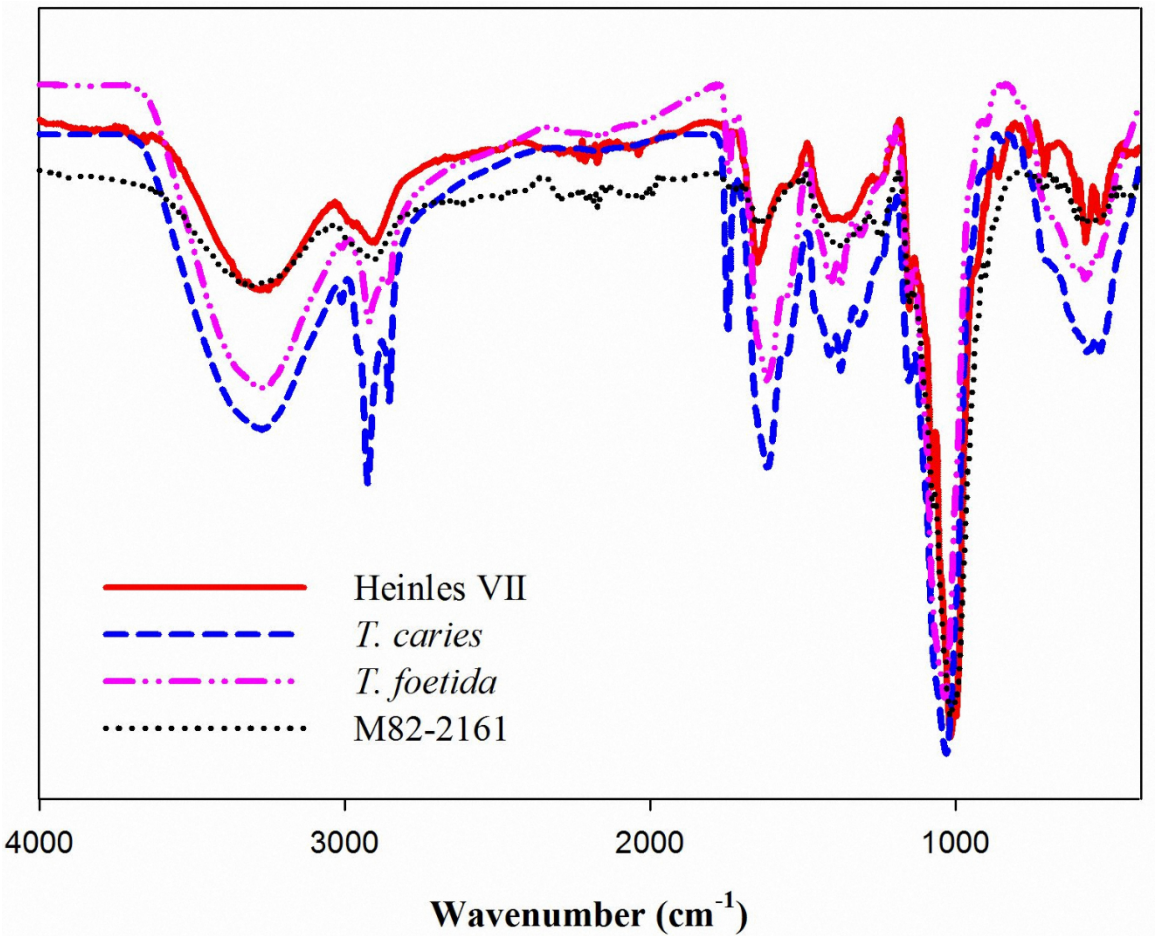

FIGURE 4
FTIR spectra of wheat and pathogen samples

TABLE 2
FTIR data of *T. foetida*, *T. caries* and host wheats (sensitive Heinles VII and resistant M82-2161)

	T. foetida	*T. caries*	Heinles VII	M82-2161
FTIR data ύ (cm^{-1})	3272,83	3265,11	3272,98	3316,09
	2880,72	2878,18	2899,42	2905,17
	1748,99	1747,52	1651,31	1654,18
	1623,17	1617,32	1150,54	1252,41
	1378,83	1376,03	1075,92	1151,97
	1157,89	1150,20	1016,78	1074,49
	1032,8	1023,67	998,44	1015,23
	724,08	579,354	711,46	902,30
	579,23	529,331	575,14	

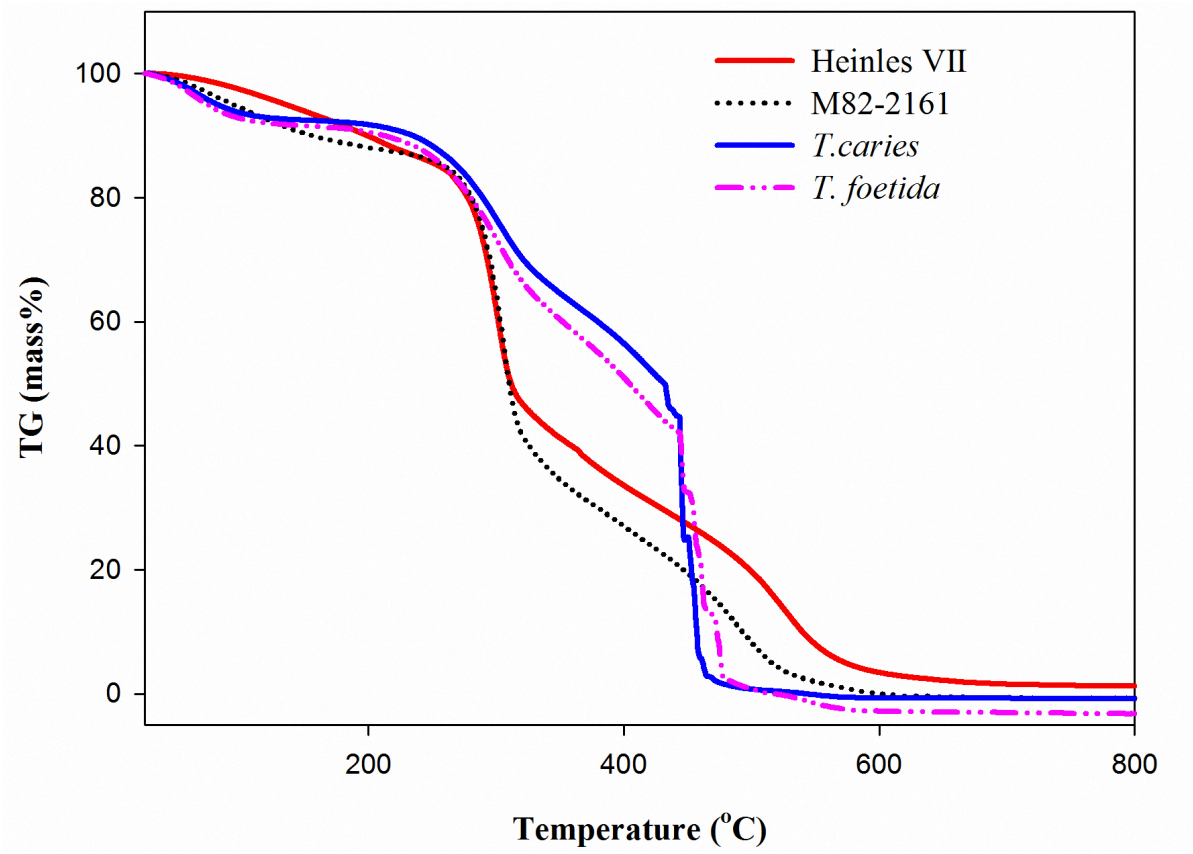

FIGURE 5
TG curves of pathogen fungi (*T. foetida* and *T. caries*) and host wheats (sensitive Heinles VII and resistant M82-2161) with a heating rate of 10°C min^{-1}

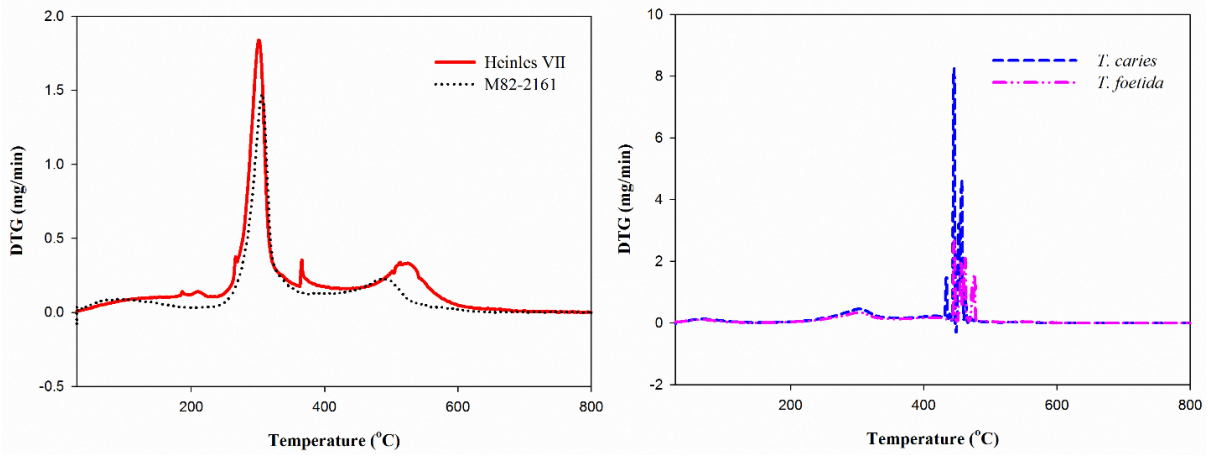

FIGURE 6
DTG curves of pathogen fungi (*T. foetida* and *T. caries*) and host wheats (sensitive Heinles VII and resistant M82-2161)

The linear heating program was conducted with heating to 800 °C. The TG curves of host wheat and pathogens were very similar among themselves. The TG spectrum of all host samples generally showed three steps. The first stage is due to evaporation. The second and third stages are degradation of cellulose, hemicellulose and non-cellulosic components, for example lignin content. These steps are different from one sample type to another. Hemicelluloses are unstable polysaccharides and decompose faster than cellulose and lignin at lower temperatures [48]. Lignin is an aromatic polymer compound and this compound is very stable and more difficult to decompose than cellulose and hemicellulose [48-50]. Blasi

(2008) reported a decomposition temperature range of hemicellulose and cellulose of 225–325 and 325–375°C, respectively [51].

Decomposition of the lignin for slow heating rates may start as early as 160°C and range up to 700°C [52]. The TG curves of Heinless VII and M82-2161 were very similar and in agreement with the literature TG curves of the samples, which showed three decomposition phases. The first and second phases were attributed to hemicellulose and cellulose decomposition, respectively. The third phase was attributed to lignin decomposition. However, the pathogens' decomposition peak arises at higher temperatures according to the host wheat. This is explained by the differences in stable organic structures in the samples. Structural and thermal decomposition temperature are interdependent. The excellent crystal structures are decomposed at high temperatures [53]. The fungal cell wall is a complex structure composed of chitin, glucans and other polymers, and there is evidence of extensive cross-linking between these components [54, 55]. The glycoproteins present in the fungal cell wall are extensively modified with both N- and O-linked carbohydrates and, in many instances, contain glycosylphosphatidyl inositol (GPI) anchors as well. The glucan component is predominantly beta-1,3-glucan, long linear chains of beta-1,3-linked glucose. Glucans having alternate linkages, such as beta-1,6-glucan, are found within some cell walls. Chitin is manufactured as chains of beta-1,4-linked N-acetyl glucosamine residues and is typically less abundant than either the glycoprotein or glucan portions of the wall. The composition of the cell wall is subject to change and may vary within a single fungal isolate depending upon the conditions and stage of growth. The glycoprotein, glucan and chitin components are extensively cross-linked together to form a complex network, which forms the structural basis of the cell wall [55].

CONCLUSION

Common bunt is a serious fungal disease affecting wheat (*Triticum aestivum L.*) production and causes economic losses in large parts of the world. *T. foetida* and *T. caries* are the most common fungal species among wheat diseases. Fungal cell walls are structurally unique and differ significantly from the cellulose-based plant cell wall. Fungal cell walls are composed of glycoproteins and polysaccharides, mainly glucan and chitin. Additional minor cell wall components are present and vary among species of fungi [55-57]. Furthermore, the plant cell wall includes such complex polysaccharides as cellulose, hemicelluloses and pectin. Upon pathogen attack, plants often deposit callose-rich cell wall appositions (i.e. papillae) at sites of attempted pathogen penetration, accumulate phenolic compounds and various toxins in the wall and synthesise lignin-like polymers to reinforce the wall [12]. All plant pathogens interact with plant cell walls [11]. Several studies have demonstrated that the roles of cell surface hydrophobicity and electrostatic charge are important in the adhesion and virulence rates of the fungal pathogens. Furthermore, adhesion is associated with the surface charge, ionic strength and hydrophobicity [17, 58-60].

Knowledge of the surface characterisation of host and pathogens makes it possible to predict how these will interact with each other or their environment. Some physicochemical and chemical properties of this interaction should be clarified. Van Loosedrecht et al. (1990) reported that the bacterial adhesion to a surface related to the hydrophobicity and charge [31]. However, they were not able to explain this bacterial adhesion by a single model [31, 58, 61]. Subsequent research has shown that the cell surface hydrophobicity is very important in adhesion [62]. The bacterial adhesion to a surface has been shown to decrease with increasing negative charge and low ionic strength. Furthermore, with increasing hydrophobicity, adhesion also tends to increase [17, 59, 60]. In this study, our SEM observations clearly exhibited the presence of surface differences between both pathogens (*T. foetida* and *T. caries*) and wheat varieties (Heinless VII and M82-2161). Our zeta analysis findings showed that both pathogenic species have a negative zeta potential. Additionally, the more-resistant wheat varieties against these pathogens have more negative zeta potentials than the sensitive wheat varieties and may cause a steric repulsion between fungus and resistant host wheat surfaces. Furthermore, *T. aestivum* species have large variations of cell surface hydrophobicity and disease rates against *Tilletia sp.* Disease rates of *Tillatia sp.* are higher at the hydrophobic substrate (Heinless VII) than the hydrophilic substrate (M82-2161). This pathogen strain adheres better to the hydrophobic substrate. We observed that the FTIR reflectance spectra of pathogens and hosts are very different. The cell structure of pathogens and host samples exhibit polyfunctionality. The TG curves of host wheat and pathogens were very similar among themselves, but the fungal pathogens decomposition peaks arise at higher temperatures depending on the host wheat. The fungal pathogens' structures may include the decomposition of molecules at higher temperatures.

The present study demonstrates that surface charge, hydrophobicity and the surface molecules' structure play very important roles for host–pathogen interactions. If the surface characterisations of host wheat and pathogens are known, the host–pathogen interaction can be better understood and future experiments can be planned for the formulation of possible important antifungal drugs and optimised growth conditions. Finally, the obtained data from this study may be used for fighting against common bunt disease in the future.

ACKNOWLEDGEMENTS

The authors would like to thank Aysel Yorgancilar from Geçitkuşağı Agricultural Research Institute (Eskişehir, Turkey) for providing of bunt isolates.

REFERENCES

[1] Lazniewska, J., Macioszek, V.K. and Kononowicz, A.K. (2012) Plant-fungus interface: The role of surface structures in plant resistance and susceptibility to pathogenic fungi. Physiological and Molecular Plant Pathology. 78, 24-30.

[2] Josefsen, L. and Christiansen, K.S. (2002) PCR as a tool for the early detection and diagnosis of common bunt in wheat, caused by *Tilletia tritici*. Mycol. Res. 106, 1287-1292.

[3] Koprivica, M., Jevtic, R. and Markovic, I.D. (2009) The Influence of *Tilletia* spp. inoculum source and environmental conditions on the frequency of infected wheat spikes. Pestic. Phytomed. 24, 185-196.

[4] Matanguihan, J.B. and Jones, S.S. (2011) A new pathogenic race of *Tilletia caries* possessing the broadest virulence spectrum of known races. Online Plant Health Progress.

[5] Dumalasova, V. and Bartos, P. (2008) Effect of inoculum doses on common bunt infection on wheat caused by *Tilletia tritici* and *T. laevis.* Czech J. Genet. Plant Breed. 44, 73-77.

[6] El-Naimi, M., Toubia-Rahme, H. and Mamluk, O.F. (2000) Organic seed-treatment as a substitute for chemical seed-treatment to control common bunt of wheat. European Journal of Plant Pathology. 106, 433-437.

[7] Waldow, F. and Jahn, M. (2007) Investigations in the regulation of common bunt (*Tilletia tritici*) of winter wheat with regard to threshold values, cultivar susceptibility and non-chemical protection measures. Journal of Plant Diseases and Protection. 114, 269-275.

[8] Zouhar, M., EvženieProkinová, J.M. and Pavelryšánek, M.V. (2010) Quantification of *Tilletia caries* and *Tilletia controvers* mycelium in wheat apical meristem by Real-time PCR. Plant Protect. Sci. 46(3), 107-115.

[9] Nagy, E. and Moldovan, V. (2007) The effect on fungicides treatments on the wheat common bunt (*Tilletia spp.)* in Transylvania. Romanian Agricultural Research. 24, 33-38.

[10] Yarullina, L.G., Kasimova, R.I., Kuluev, B.R., Surina, O.B., Yarullina, L.M. and Ibragimov, R.I. (2014) Comparative study of bunt pathogen resistance to the effects of fungicides in callus co-cultures *Triticum aestivum* with *Tilletia caries.* Agricultural Sciences. 5, 906-912.

[11] Vorwerk, S., Somerville, S. and Somerville, C. (2004) The role of plant cell wall polysaccharide composition in disease resistance. Trends in Plant Science. 9(4), 203-209.

[12] Hematy, K., Cherk, C. and Somerville, S. (2009) Host–pathogen warfare at the plant cell wall. Current Opinion in Plant Biology. 12, 406-413.

[13] Hayashi, H., Seiki, H., Tsuneda, S. and Hirata, A., Sasaki H. (2003) Influence of growth phase on bacterial cell electrokinetic characteristics examined by soft particle electrophoresis theory. Journal of Colloid and Interface Science. 264, 565-568.

[14] Fan, H.Y., Nazari, M., Raval, G., Khan, Z., Patel, H. and Heerklotz, H. (2014) Utilizing zeta potential measurements to study the effective charge, membrane partitioning, and membrane permeation of the lipopeptide surfactin. Biochimica et Biophysica Acta. 1838, 2306-2312.

[15] Schmitt, J. and Flemming, H.C. (1998) FTIR-spectroscopy in microbial and material analysis. International Biodeterioration and Biodegradation. 41, l-11.

[16] Marshall, K.C. and Mozes, N. (1991) The importance of studying microbial cell surfaces. In: Handley, P.S., Busscher, H.J., Rouxhet, P.G. (eds.) Microbial Cell Surface Analysis. VCH Publisher, New York, 3-19.

[17] Singh, T., Saikia, R., Jana, T. and Arora, D.K. (2004) Hydrophobicity and surface electrostatic charge of conidia of the mycoparasitic *Trichoderma* species. Mycological Progress, 3(3), 219-228.

[18] Hazen, K.C., Lay, J.G., Hazen, B.W., Fu, R.C. and Murthy, S. (1990) Partial biochemical characterization of cell surface hydrophobicity and hydrophilicity of *Candida albicans*. Infection and Immunity. 58, 3469-3476.

[19] Biodochka, M.J., Leger, S.T., Joshi, R.J. and Roberts, D.W. (1995) The rodlet layer from aerial and submerged conidia of the entomopathogenic fungus *Beauveria bassiana* contains hydrophobin. Mycological Research. 99, 403-406.

[20] Hazen, K.C. and Hazen, B.W. (1992) Hydrophobic surface protein masking by the opportunistic fungal pathogen *Candida albicans*. Infection and Immunity. 60, 1499-1508.

[21] Jeffs, L.B. and Khachatourians, G.G. (1997) Estimation of spore hydrophobicity for members of the genera *Beauveria, Metarhizium* and *Tolypocladium* by salt-mediated aggregation and sedimentation. Canadian Journal of Microbiology. 43, 23-28.

[22] Wessels, J.G.H. (1997) Hydrophobins: Proteins that change the nature of the fungal surface. Advance Microbiology and Physiology. 38, 1-45.

[23] Wessels, J.G.H. (1999) Fungi in their own right. Fungal Genetics and Biology. 27, 134-145.

[24] Sutandar, P., Ahn, D.J. and Franses, E.I. (1994) FTIR ATR analysis for microstructure and water uptake in poly (methyl methacrylate) spin cast and Langmuir–Blodgett thin films. Macromolecules. 27, 7316-7328.
[25] Hansen, M.A.T., Kristensen, J.B., Felby, C. and Jørgensen, H. (2011) Pretreatment and enzymatic hydrolysis of wheat straw (*Triticum aestivum* L.) – The impact of lignin relocation and plant tissues on enzymatic accessibility. Bioresource Technology. 102, 2804-2811.
[26] Jeguirim, M., Dorge, S. and Trouvé, G. (2010) Thermogravimetric analysis and emission characteristics of two energy crops in air atmosphere: *Arundo donax* and *Miscanthus giganthus*. Bioresource Technology. 101, 788-793.
[27] Carrier, M., Loppinet-Serania, A., Denux, D., Lasnier, J.M., Ham-Pichavant, F., Cansell, F. and Aymonier, C. (2011) Thermogravimetric analysis as a new method to determine the lignocellulosic composition of biomass. Biomass and Bioenergy. 35, 298-307.
[28] Chen, W.H. and Kuo, P.C. (2011) Isothermal torrefaction kinetics of hemicellulose, cellulose, lignin and xylan using thermos gravimetric analysis. Energy. 36, 6451-6460.
[29] Mosse, B. and Jones, G.W. (1968) Surface features of fungal spores as revealed in a scanning electron microscope trans. Br. Mycol. Soc. 51, 3-4.
[30] Shi, Y.L., Loomis, P., Christian, D., Carris, L.M. and Leung, H. (1996) Analysis of the genetic relationship among the wheat bunt fungi using RAPD and ribosomal DNA markers. Phytopathology. 86, 311-318.
[31] Van Loosdrecht, M.C.M., Norder, W., Lyklema, J. and Zehnder, A.J. (1990) Hydrophobic and electostatic parameters in bacterial adhesion. Aquat. Sci. 51, 103-114.
[32] Gierlinger, N., Goswami, L., Schmidt, M., Burgert, I., Coutand, C. and Rogge, T. (2008) In situ FT-IR microscopic study on enzymatic treatment of poplar wood cross-sections. Biomacromolecules. 9(8), 2194-2201.
[33] Pandey, A. (1990) Improvement in solid-state fermentation for glucoamylase production. Biological Wastes. 34(1), 11-19.
[34] Shang, L., Ahrenfeldt, J., Holm, J.K., Sanadi, A.R., Barsberg, S., Thomsen, T., Stelte, W. and Henriksen, U.B. (2012) Changes of chemical and mechanical behavior of terrified wheat straw. Biomass and Bioenergy. 40, 63-70.
[35] Farooq, U., Khan, M.A., Athar, M. and Kozinski, J.A. (2011) Effect of modification of environmentally friendly biosorbent wheat (*Triticum aestivum*) on the biosorptive removal of cadmium(II) ions from aqueous solution. Chemical Engineering Journal. 171, 400-410.
[36] Faix, O. (1991) Classification of lignins from different botanical origins by FT-IR spectroscopy. Holzforschung. 45, 21-27.
[37] Hansen, M.A.T., Jørgensen, H., Laursen, K.H., Schjoerring, J.K. and Felby, C. (2013) Structural and chemical analysis of process residue from biochemical conversion of wheat straw (*Triticum aestivum* L.) to ethanol. Biomass and Bioenergy. 56, 572-581.
[38] Donohoe, B.S., Decker, S.R., Tucker, M.P., Himmel, M.E. and Vinzant, T.B. (2008) Visualizing lignin coalescence and migration through maize cell walls following thermochemical pretreatment. Biotechnol Bioeng. 101(5), 913-925.
[39] Pandey, K. (1999) A study of chemical structure of soft and hardwood and wood polymers by FTIR spectroscopy. J Appl Polym Sci. 71(12), 1969-1975.
[40] Kristensen, J.B., Thygesen, L.G., Felby, C., Jørgensen, H. and Elder, T. (2008) Cell-wall structural changes in wheat straw pretreated for bioethanol production. Biotechnol Biofuels. 1(5), 1-9.
[41] Akerholm, M., Hinterstoisser, B. and Salmen, L. (2004) Characterization of the crystaline structure of cellulose using static and dynamic FT-IR spectroscopy. Carbohyd. Res. 339, 569-578.
[42] Demir, P., Onder, S. and Severcan, F. (2015) Phylogeny of cultivated and wild wheat species using ATR–FTIR spectroscopy. Spectrochimica Acta Part A: Molecular and Biomolecular Spectroscopy. 135, 757-763.
[43] Gorgulu, S.T., Dogan, M. and Severcan, F. (2007) The characterization and differentiation of higher plants by Fourier transform infrared spectroscopy. Appl. Spectrosc. 61, 300-308.
[44] Naumann, D. (2000) Infrared spectroscopy in microbiology. In: Meyers, R.A. (ed.) Encyclopedia of Analytical Chemistry. John Wiley and Sons Ltd., Chichester, 102-131.
[45] Robert, P., Marquis, M.L., Barron, C.C., Guillon, F. and Saulnier, L. (2005) FT-IR investigation of cell wall polysaccharides from cereal grains. Arabinoxylan infrared assignment. J. Agr. Food Chem. 53, 7014-7018.
[46] Saulnier, L., Robert, P., Grintchenko, M., Jamme, F., Bouchet, B. and Guillon, F. (2009) Wheat endosperm cell walls: spatial heterogeneity of polysaccharide structure and composition using micro-scale enzymatic fingerprinting and FT-IR microspectroscopy. J. Cereal Sci. 50, 312-317.
[47] Greenhalf, C.E., Nowakowski, D.J., Bridgwater, A.V., Titiloye, J., Yates, N., Riche, A. and Shield, I. (2012) Thermo chemical characterisation of straws and high yielding perennial grasses. Industrial Crops and Products. 36, 449-459.

[48] Burhenne, L., Messmer, J., Aicher, T. and Laborie, M.P. (2013) The effect of the biomass components lignin, cellulose and hemicellulose on TGA and fixed bed pyrolysis. Journal of Analytical and Applied Pyrolysis. 101, 177-184.
[49] Gani A. and Naruse, I. (2007) Effect of cellulose, lignin content on pyrolysis and combustion characteristics for several types of biomass. Renewable Energy. 32, 649-661.
[50] Pandey, M.P. and Kim, C.S. (2011) Lignin depolymerization and conversion: a review of thermochemical methods. Chemical Engineering and Technology. 34, 29-41.
[51] Blasi, C.D. (2008) Modeling chemical, physical processes of wood and biomass pyrolysis. Progress in Energy and Combustion Science. 34, 47-90.
[52] Alwani, M.S., Abdul Khalil, P.S.H., Sulaiman, O., Islam Md, N. and Dungani, R. (2014) An approach to using agricultural waste fibres in biocomposites application: thermogravimetric analysis and activation energy study. BioResources. 9(1), 218-230.
[53] Ouajai, S. and Shanks, R.A. (2005) Composition, structure and thermal degradation of hemp cellulose after chemical treatments. Polym. Degrad. Stab. 89(2), 327-335.
[54] Adams, D.J. (2004) Fungal cell wall chitinases and glucanases. Microbiology. 150, 2029-2035.
[55] Bowman, S.M. and Free, S.J. (2006) The structure and synthesis of the fungal cell wall. BioEssays. 28, 799-808.
[56] Keskin, A.C., Acik, L., Araz, A. and Guler, P. (2016) Genetic identification for some *Fusarium spp*. using random amplified polymorphic DNA polymerase chain reaction (RAPD-PCR) technique. Fresen. Environ. Bull. 25, 5611-5617.
[57] Pieczul, K., Horoszkiewicz-Janka, J., Perek, A. and Świerczyńska, I. (2015) The risk of production of mycotoxins incereal grains by the chemotypes of *Fusarium spp.* Fresen. Environ. Bull. 24, 2527-2533.
[58] Hazen, K.C. and Glee, P.M. (1994) Hydrophobic cell wall protein glycosylation by the pathogenic fungicides *Candida albicans*. Canadian Journal of Microbiology. 40, 266-272.
[59] Jeffs, L.B., Xavier, I.J., Mattai, R.E. and Khachatoutians, G.G. (1999) Relationships between fungal spore morphologies and surface properties for entomorphogenic members of the genera *Beauveria*, *Metarhizium*, *Tolypocladium* and *Verticillium.* Canadian Journal of Microbiology. 45, 936-948.
[60] Neu, T.R. (1996) Significance of bacterial surface-active compounds in interaction of bacteria with interfaces. Microbiological Review. 60, 151-166.
[61] Van Loosdrecht, M.C.M., Lyklema, J., Norde, W., Schraag, G. and Zehnder's, J.B. (1987) The role of bacterial cell wall hydrophobicity in adhesion. Applied and Environmental Microbiology. 53(8), 1893-1897.
[62] Li, B. and Logan, B.E. (2004) Bacterial adhesion to glass and metal-oxide surfaces. Colloids and Surfaces B: Biointerfaces. 36, 81-90.

Received: **21.09.2017**
Accepted: **06.06.2018**

CORRESPONDING AUTHOR

Ismail Poyraz
Department of Molecular Biology and Genetic,
Faculty of Science and Letters,
Bilecik Seyh Edebali University,
11230 Bilecik – Turkey

e-mail: ismail.poyraz@bilecik.edu.tr